Comparison of neutron and ion irradiation induced lattice parameter changes in Ni and MgO single crystals

Xin Jin, Alexandre Boulle, Jérôme Bourcoit, Aurélien Debelle

Comparison of neutron and ion irradiation induced lattice parameter changes in Ni and MgO single crystals

Xin JIN[1,2], Alexandre BOULLE[2], Jérôme BOURCOIS[1], Aurélien DEBELLE[1]

1. Université Paris-Saclay, CNRS/IN2P3, Institut de Physique des 2 Infinis Irène Joliot-Curie, ICJLab, 91405 Orsay, France
2. IRCer, CNRS UMR 7315, Centre Européen de la Céramique, 12 rue Atlantis, 87068 Limoges Cedex, France

Data, available in the literature, of lattice parameter changes (i.e. elastic strain) in Ni and MgO single crystals neutron-irradiated in nuclear reactors are tentatively reproduced using *ad hoc* ion irradiation experiments. The nature and energy of the ions were selected so that their weighted average recoil spectrum matches at best that of the neutron spectrum inside the reactor. The ion fluence was calculated to obtain similar displacement per atom (dpa) levels. The lattice parameters of the irradiated samples were determined using high-resolution X-ray diffraction. We show that, for Ni, it is not possible to reproduce the neutron data because no lattice parameter change is measured after ion irradiation. Main reasons for this failure are the low dpa levels, the small damaged volume and the presence of a complex defect spectrum that leads to a net zero strain. On the contrary, for MgO, which is more prone to exhibiting high strain levels upon irradiation, a very close lattice parameter change buildup is obtained between neutron and ion irradiations, providing that the ion irradiation temperature is significantly increased (by ~473 K).

I. Introduction

The understanding of radiation effects in materials has gained a lot from the study of nuclear materials because, as these later are inherently submitted to various irradiation sources, the study of their behavior under harsh radiative environments was, and remains an important topic to tackle. The major issue with respect to particle irradiation for nuclear materials is neutron irradiation. In order to investigate the effects of this type of irradiations, there are two options. The first one is to use test reactors that reproduce, quite closely, actual conditions experienced in commercial reactors. The second option lies in the use of ion beams delivered by particle accelerators. Pros and cons of these two alternatives have been recently addressed in a review paper [1] and also in [2-3] and it is not in the scope of the current paper to make such a detailed comparison. For decades, numerous works have been carried out to theorize on the simulation of neutron damage by ion irradiation. The reader can refer to [4-5] and references therein to find more information about fundamental and practical concepts. Despite this extensive work, the question of the validity of ion irradiation as a surrogate to neutron irradiation is still debated. As an evidence of this statement, we can mention an ongoing research work of the International Atomic Energy Agency (IAEA) named "Accelerator Simulation and Theoretical Modelling of Radiation Effects - SMoRE-II". One of the objectives of this program is to quantify the degree of agreement between microstructures generated by ion and neutron irradiation. Indeed, there are various discrepancies between the two methods, particularly in the damage characteristics such as its volume, its creation rate, its homogeneity, etc… (the most important issues related to ion irradiation experiments are addressed in section III of the current paper). These differences can lead to significantly different microstructures whereas the ion irradiation method is supposed to be a proxy for neutron irradiation. Nevertheless, it has been shown in several cases that the former can allow reproducing phenomena (e.g. swelling, creep, radionuclides production) occurring during the latter in fission and fusion reactors [1,6-8]. Therefore, one can expect that the corresponding microstructural features are also identical, which is sometimes the case [9-11], but not always [12-13]. In fact, it is usually impossible for ion irradiation experiments to simultaneously achieve all aspects of microstructural changes occurring under neutron irradiation [2,10]. In conclusion, the answer to the above-mentioned question is not straightforward.

In the current paper, we aim at providing a piece of answer to that very question. For this purpose, we used a simple strategy. We first collected, in the literature, data of lattice parameter changes (i.e. elastic strain build-up) in neutron-irradiated single crystals. The selection, voluntarily limited to one case for both materials (because of the high number of experiments required to reproduce those data), was essentially based on two major criteria: the availability of the characteristics of the neutron spectrum and the availability of data for single-crystals. Then, we carried out targeted ion irradiation experiments, followed by high-resolution X-ray diffraction (HR-XRD)

measurements, to determine the corresponding strain build-ups. We show hereafter that even such a 'simple' comparison between strain kinetics from neutron and ion irradiation experiments is not direct.

II. Experimental details

Ni and MgO single crystals were purchased at MTI corporation in Richmond, CA, USA. Purity of Ni was > 99.99 % and that of MgO was > 99.95 %. Lattice parameters (at room-temperature) of pristine samples were found to be those of the pure, perfect materials, i.e. 0.35295 nm and 0.42160 nm for Ni and MgO, respectively. Samples were mirror-polished (see details on the MTI website) with a very weak surface roughness (< 0.1 nm), i.e. much lower than the ion projected ranges (see hereafter).

Ion irradiation experiments were conducted on the JANNuS-SCALP platform of the IJCLab. All series of irradiations (except for some previously performed Au irradiations) were carried out at room temperature (RT). Details of the ion energies, fluences and ranges are provided, when needed, in sub-sections of section IV. Note that the selection of the ion species and energies was made based on the capacities of the ion accelerators, and also considering potential interactions between implanted ions and the target (see section III). Tables I and II list the irradiations details.

High-resolution X-ray diffraction measurements were performed on two equivalent equipment whose details are provided in [14]. Briefly, we used both a bent multilayer mirror and a monochromator to have an intense, parallel and monochromatic (Cu-$K_{\alpha 1}$) radiation. We performed regular, symmetric (so-called θ-2θ) scans that allow recording the signal from both the irradiated and unirradiated parts of the crystals, which is convenient because we thus have the two corresponding Bragg peaks and hence, the possibility to accurately estimate the lattice strain, as demonstrated in [15] and references therein. We want to mention here that we used high-resolution configurations for all measurements to ensure to detect the smallest peak shift (or rather, peak splitting). The minimum scattering angle for two close peaks to be both detected essentially depends on the peak widths, on the probed hkl reflection and on the disorder level. For the current conditions, we had a resolution, expressed in terms of lattice strain, of 0.01 %, as estimated by a systematic study with the RaDMaX-online program [16].

III. Methodology

In order to carry out this 'simple' comparison, we had to develop a complete methodology to take into account some important characteristics, biases and drawbacks of ion irradiation experiments as compared to neutron irradiations (most of which are documented in [2], and recently further illustrated in [17]). Four major points were considered: (i) the most common artifacts (injected ions and free surfaces), (ii) the recoil spectra, (iii) the quantification of the dose exposure and the dose rate effect, and (iv) the anisotropy of the damaged volume.

III.1. Artifacts of ion irradiations

Several artefacts related to (low-energy) ion irradiation experiments must be considered, among which the presence of free surfaces. These latter include grain boundaries and the sample surface itself that strongly affect the defect diffusivity when only a thin layer of a bulk sample is irradiated. Those free surfaces act as efficient defect sinks, leading sometimes to defect-denuded zones. In our work, we used single-crystals, which allows ruling out grain-boundary effects. Regarding the sample surface, using rate theory (as explained in [2]), we could estimate the width of the denuded zones. For irradiations of both Ni and MgO, a value in the order of 0.5 nm was found (considering vacancy migration energies of 1.2 eV and 2.1 eV for Ni [18] and (Mg in) MgO [19], respectively). This small width shows that the surface effect can be disregarded here, particularly as we estimated the lattice strain at the damage peaks located around 25 and 500 nm.

Injected species, either impurities or self-ions, are also known to affect many processes like void swelling, phase transformation and precipitation [2]; this issue was already put forward in the early 1980's [20]. In the current work, a maximum of 15 appm was used for irradiations of Ni crystals, which is extremely low as compared to concentrations where significant effects of those injected species are observed (see the illustrative example in Fe-Cr alloys [21]). For irradiations of MgO, maximum Au and I concentrations of 200 and 80 appm were used, respectively, which is higher than for Ni. Nevertheless, only species like transition metals [22] (which, depending on their electronic configuration, can be incorporated in either interstitial or substitutional sites [23]), but also Rb and Nb [24] have been shown to influence the microstructure changes during ion irradiation of MgO. Au ions are known to form nanoclusters in MgO only upon very specific conditions [25] which are not fulfilled here; regarding I ions, even with a concentration of 120 appm, no effect of their presence on the resulting microstructure has been observed [26]. Therefore, we can reasonably assume that the effect of the injected species can be disregarded in the current work.

III.2. Weighted average recoil spectra

In neutron irradiations, the energy transferred by the neutrons to a target material atom, usually referred to as the Primary Knock on Atom (PKA) or recoil, can be sufficient (if it exceeds the threshold displacement energy, E_d) to displace this atom. If this latter has enough energy, it can in turn displace other target atoms, giving rise to a collision cascade and the total number of displaced atoms depends on the PKA energy [27-30]. All the displaced atoms then evolve and a fraction of them produce (clusters of) defects that modify the material properties. Therefore, in order to accurately describe the neutron-target interactions, it is important to look at the PKA spectrum. More relevantly, the weighted average recoil spectrum (WARS) should be considered, as it allows getting a reasonable description of the defect production process, weighing the primary recoil spectrum by the damage energy produced

in each recoil event [27,31]. The median energy, $T_{1/2}$, which is the energy for which half of the recoils are generated in cascades with energies greater than $T_{1/2}$ (and half with energies lower), is frequently used as a sound parameter to describe a given particle-solid interaction process [30]. Even though both the WARS and the median energy do not provide a complete description of the recoil spectrum, they undeniably carry more information than the sole estimation of the number of displaced atoms. Besides, the choice of the ion nature and energy can be made so that the corresponding WARS matches that of the neutron spectrum inside a given reactor. This is precisely what we mean by "targeted irradiations" (see Introduction).

In order to calculate the WARS corresponding to a neutron spectrum, we used the DART code (whose detailed description is given in [32]). Briefly, this code was created to estimate the PKA spectra produced in a polyatomic solid target. The neutron cross-sections are directly extracted from neutron libraries for each isotope (ENDF /B VI in the standard version), and in order to take into account resonances in the differential neutron isotope cross-section, a multi group approach was chosen to compute the PKA spectrum. The nuclear reactions are also considered (as the one taking place with Ni, see below). The DART code treats ion-solid interactions within the Binary Collision Approximation (BCA) framework [33, 34]. For the nuclear stopping, the repulsive Thomas-Fermi interatomic potential was used and for the electronic stopping, the Ziegler formalism was implemented. The WARS is one of the direct output files of DART. An example is given in Fig.1 that displays, in particular, the spectrum corresponding to the Russian nuclear reactor IVV-2M, using E_d(Ni) = 40 eV [35] (note that this is the recommended value, but in fact, the actual absolute value is meaningless as long as we use the same one for ion-target and neutron-target interaction simulations). For this reactor, the median energy, $T_{1/2}$, is 57.3 keV. It is worth mentioning that we included the nuclear reactions occurring between ^{58}Ni and ^{59}Ni isotopes and thermal neutrons, which is why we used the entire neutron spectrum of the reactor (this spectrum is shown in Appendix A).

To calculate the WARS of an ion-target experiment, we used SRIM, which is an extremely well-known package of codes designed for computing any ion-target interaction, so we will not present it here; details can be found in [36]. It is however important to mention that, if the WARS is a direct output of DART, it is not the case for SRIM. In order to obtain such a spectrum, one needs to process the (heavy) text file named "collisions.txt". We wrote a Python script that allows taking this file as an input and getting the WARS as an output (the Python file is provided as supplementary data).

In addition to the WARS corresponding to the IVV-2M nuclear reactor, Figure 1 presents three WARS corresponding to 600 keV $^{58}Ni^{+}$ ions interacting with a nickel target: one spectrum was obtained with the DART code while the two others come from SRIM using the two options "Quick calculations, or Kinchin-Pease, KP" and "Full Damage cascades, FD". There is almost no difference between these two latter spectra (which is expected, given the definition of the WARS), whereas that derived from

DART exhibits a significant discrepancy. This difference comes from the fact that DART only uses the initial incident ion energy to solve the analytical equations giving the WARS (which makes sense for neutrons), but SRIM follows the projectile all along its path and takes into account its slowing-down (which is sound for ions). Consequently, the whole spectrum derived from SRIM is shifted towards lower energies, i.e. the spectrum is softer, as compared to DART. In the following, to determine the WARS, we use DART for neutron-target interactions and SRIM for ion-target interactions.

III.3. Damage dose and dose rate effect

Another important parameter to consider when comparing ion and neutron irradiation experiments is the "exposure dose", or damage dose. There exist discrepancies between the number of displaced atoms (estimated within the BCA, like with the KP model for instance) and the actual defect density (experimentally measured or determined by simulation methods); this issue is well documented [28,30]. The quantification of surviving defects really requires a huge amount of experimental and/or computational efforts [27-30,37-38]. This difficulty prevents from using the defect density as a simple, common parameter to compare irradiation experiments. The fluence does not appear as a relevant parameter either, as it does not integrate the displacement cross-section nor does it describe the collision characteristics. We thus used the displacement per atoms (dpa) parameter (even though a new concept has recently emerged, the arcdpa [38], that we do not use here because it requires a lot of fundamental data to be used). For DART calculations, the neutron spectrum is known and the dpa production rate is an output value. Note that the estimation of the number of displaced atoms does not rely on the Kinchin-Pease formalism [39] in DART, it is based on the Lindhard formalism [40]. Therefore, for SRIM, the calculation of the dpa was derived from the 'collision events' distributions determined in the FD mode (we used the dpa at the damage peak, because we determined the lattice strain in this region, see sect. III.4.). We are aware that there exists a controversy on the 'correct' way to estimate the dpa values with SRIM [41-43]. However, in the present work, we only needed a damage parameter that could be used for both ion and neutron irradiation experiments, irrespective of its actual significance and of its potential agreement with actual defect concentrations. Consequently, in both cases, the dpa values were based on the number of displaced atoms, a quantity that we did specifically calculate ourselves for each (ion or neutron) irradiation condition.

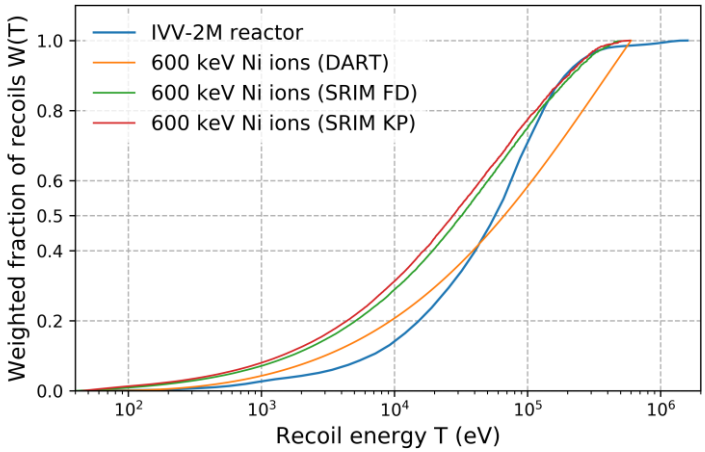

Figure 1: Weighted average recoil spectra corresponding to the neutron spectrum of the IVV-2M reactor and to 600 keV Ni^+ ions. Calculations were performed with either DART [32] or SRIM [36] in "Full damage, FD" or "Kinchin-Pease, KP" modes, as indicated in the legend.

Another major difference between neutron and ion irradiation experiments lies in the dose rate, or rather, the damage rate [1-2,17]. Indeed, dpa rates in nuclear reactors are several orders of magnitude lower than those usually obtained with ion accelerators. This issue can be resolved using the invariance theory derived by Mansur [4]. This theory states that a change in an irradiation parameter between the nuclear reactor and the ion accelerator can be accommodated by a shift in another parameter. For the dpa rate, a shift in temperature is usually applied (see [2] and references therein). However, this temperature shift must be (most of the times) estimated *a posteriori* (i.e. after a trial and error process to eventually reproduce the desired microstructural features). For this reason, we decided to keep, for ion irradiations, the temperature used in the reactor, i.e. RT.

III.4. Determination of the lattice parameter change in irradiated surface layers

While neutron irradiation leads to homogeneous damage of the bulk materials, ion irradiation, particularly at the energies used in this work, alter only thin layers at the sample surface, typically a few hundreds of nm here. One can consider this system as a thin layer deposited onto a substrate (of the same nature). This layer is thus free to swell or shrink only along the surface normal direction because there exists an in-plane constraint from the thick, rigid unirradiated part of the material. The resulting strain/stress state exhibited by the layer is therefore anisotropic, and the measured strain levels cannot be directly compared with those obtained for neutron-irradiated samples. For this drawback to be overcome, one must use an adapted mechanical description, which we did use here. Such a description has already been presented elsewhere, and has proven to be valid [44-45]. In short, with this method, one can calculate, from the measured strain, the strain that would have experienced the irradiated layer if it were free to change its dimensions in the three space directions.

IV. Results and discussion

IV. 1. Ni target in the IVV-2M REACTOR

In 2016, a paper was published that presented the lattice parameter change in Ni single crystals irradiated in the IVV-2M Russian reactor (see [46] and Fig.1 in Appendix B). The neutron doses and irradiation temperature used in that work could not lead to the void swelling regime, which was a prerequisite for the current work. The measured lattice parameter change was, for instance, similar to that determined in electron-irradiated Ni crystals at 6 K [47]. We decided to try to reproduce these data performing ion irradiation experiments. In Fig.2 is presented the WARS corresponding to this nuclear reactor. In order to get a WARS with ions as close as possible to that one, while introducing an extremely low quantity of impurities (maximum 15 appm), we used 300 keV Bi^{2+} ions. Yet, as the corresponding damaged thickness was very limited (see dpa depth profile in Fig. 3), we also used 600 keV (self) Ni^{+} ions (with, also, a maximum of 15 appm). For this second condition, the WARS is, conveniently, slightly harder ($T_{1/2}$ is 27.6 keV as compared to 25 keV for 300 keV Bi^{2+} ions and to 57.3 keV for the neutrons), and the damaged thickness is significantly increased, from 0.05 µm to 0.35 µm. Table I summarizes these irradiation conditions.

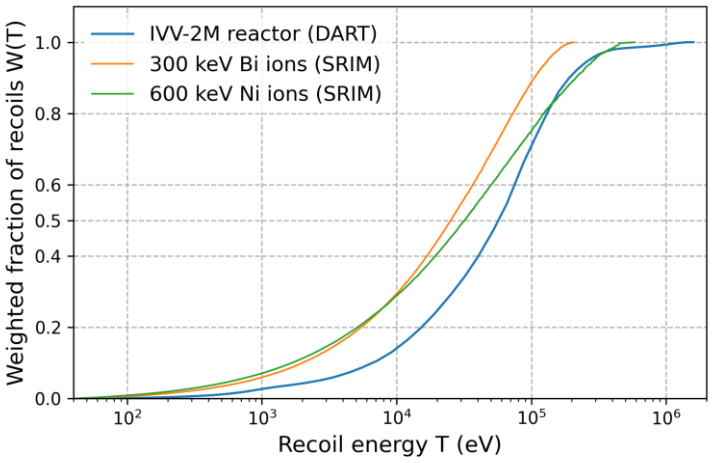

Figure 2: Weighted average recoil spectra corresponding to the neutron spectrum of the IVV-2M reactor and to 600 keV Ni^{+} and 300 keV Bi^{2+} ions; the target is Ni.

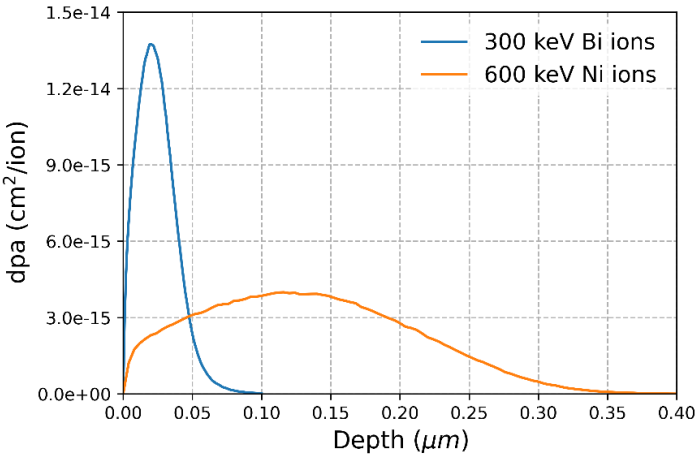

Figure 3: Dpa depth distributions corresponding to the two conditions implemented for the ion irradiations of the Ni single crystals. Calculations were performed with SRIM [36] in the FD mode.

XRD results for Bi and Ni irradiations are presented in Fig.4(a) and Fig.4(b), respectively. Clearly, no lattice parameter change is detectable for Bi irradiations, as no peak shift is observed (see the vertical dotted line that indicates the position of the Bragg peak for pristine Ni crystals in Fig. 4(a)). After significantly increasing the damage thickness with the Ni irradiations and also doubling the dpa level (with respect to the maximum dpa inside the reactor), this result still holds (Fig. 4(b)). Only diffuse scattering due to the presence of extended defects is observed, similarly to what was recently reported in ion-irradiated Ni crystals [48]. The lattice parameter change measured after neutron irradiation was very weak (see Appendix B and [46]), but given our experimental resolution, we should have been able to detect such low strain levels, at least at high dpa and for the Ni irradiations, for which the damaged thickness is ~350 nm. This statement is based on simulations of XRD curves using the RaDMaX-online program which is dedicated to retrieving strain depth profiles in irradiated materials [16]. But it could have been anticipated to not measure any strain, as some of the current authors obtained similar results in another work on ion-irradiated Ni single crystals [49]. In that work, a dpa level of ~0.13 was reached and the damaged thickness was ~4 µm. Even in that case, no elastic strain was detected. The main reason invoked for this finding was the presence of a complex spectrum of defects, including vacancy-type clusters and both interstitial Frank and perfect dislocation loops, the combination of which was leading to that zero net strain. In [47] (the work mentioned at the beginning of this section), the annealing behavior of the electron-irradiated Ni samples was studied, and such a complex distribution of defects was also put forward. Additionally, in their work, after an annealing at 300 K (the current irradiation temperature), only 10 % of the initial (i.e. measured at 6 K) lattice parameter change was measured, so a strain of 0.003 %, impossible to detect with our experimental conditions. Therefore, even though the actual microstructure of the ion-irradiated Ni crystals might be similar to that produced after neutron irradiation, different characterization techniques such as transmission

electron microscopy or atomic probe tomography should be used to proceed to that comparison. The monitoring of the lattice parameter, which has the advantage of being achievable without any sample preparation, is therefore not appropriate in the current case. More generally, it is obviously not suited to situations where materials develop low strain levels under irradiation, which is the case of most of the pure (bulk) metals irradiated at RT and above. In fact, we adopted the same methodology for Cu, to reproduce the results of [50], but we did not measure any irradiation-induced strain (here also, as for Ni, a very low strain level was expected). To moderate the statement of the inapplicability of this methodology to metals, we must point out that it could be valid for some metallic alloys, as, for example, NiFe and NiFeCo (see [49]). More generally, it could be applied to materials exhibiting large strain values when subjected to irradiation [51,52]. This is the case for instance for many semiconductors and for some ceramics, like magnesium oxide, MgO, which is dealt with hereafter.

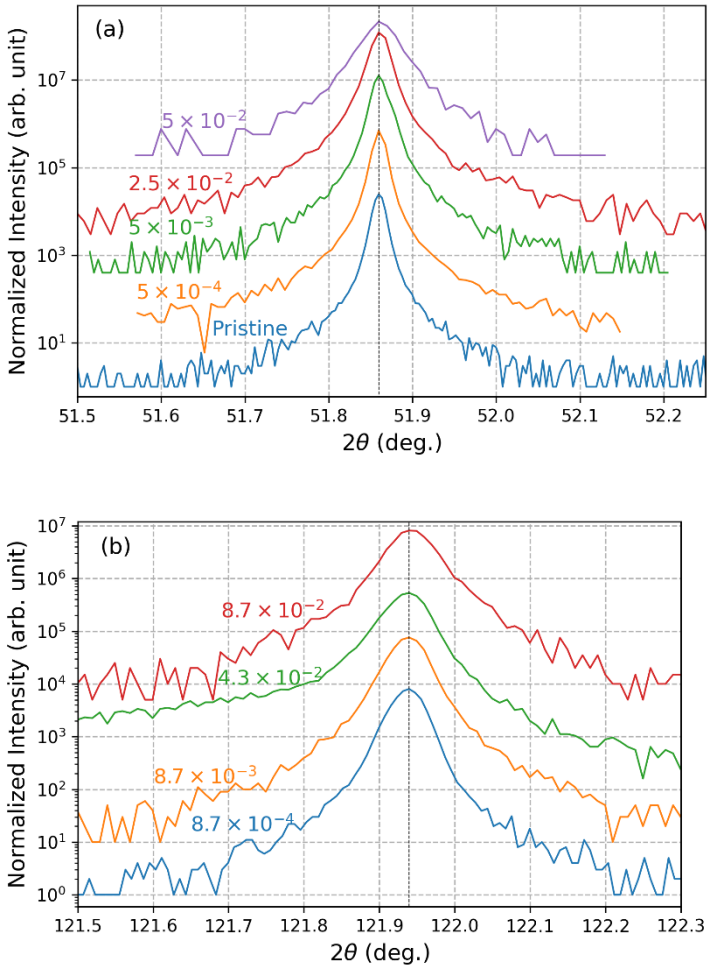

Figure 4: XRD curves of Ni single crystals irradiated with a) 300 keV Bi^{2+} ions and b) 600 keV Ni^{+} ions at the indicated dpa. The vertical dotted lines indicate the position of the Bragg peaks for the pristine crystal. Curves are stacked for visualization purposes.

IV.2. MgO target in the DIDO REACTOR

In 1971, a work presenting the change in the lattice parameter of MgO single crystals irradiated in the Harwell DIDO reactor [53] was published. We decided to reproduce these data performing ion irradiation experiments. In Fig.5 are presented the WARS corresponding to the nuclear reactor, along with the one determined for 4 MeV Au^{2+} ions; we used $E_d(Mg) = E_d(O) = 60$ eV [54]. The corresponding $T_{1/2}$ are 64.6 keV and 26.8 keV, respectively. Clearly, the WARS related to the 4 MeV Au ions is too soft, but it seems to be the hardest one we can produce (this statement is the result of a series of WARS calculations with many ion nature/energy combinations). In Fig.5 are also plotted two other WARS we used for data comparison: that of 1.2 MeV Au^+ ions (because we already had a significant amount of data regarding MgO crystals irradiated with these ions at several temperatures above RT), and that of 1 MeV Ne^+ ions (for comparison with [55]). Lastly, the WARS of 1.5 MeV I^+ is presented in Fig.5. It is almost identical to that of 1.2 MeV Au^+ ions (with $T_{1/2}$ ~18.5 keV for both), but, important to mention, iodine irradiations were performed at RT while 1.2 MeV Au^+ irradiations were carried out above RT. Note that the WARS for I^+ ions is close to that of the 4 MeV Au^{2+} ions, which will be of relevance for the following data interpretation. All dpa depth distributions corresponding to the above-mentioned ion irradiation conditions are presented in Fig.6, and the dpa levels and ion fluences are summarized in Table II.

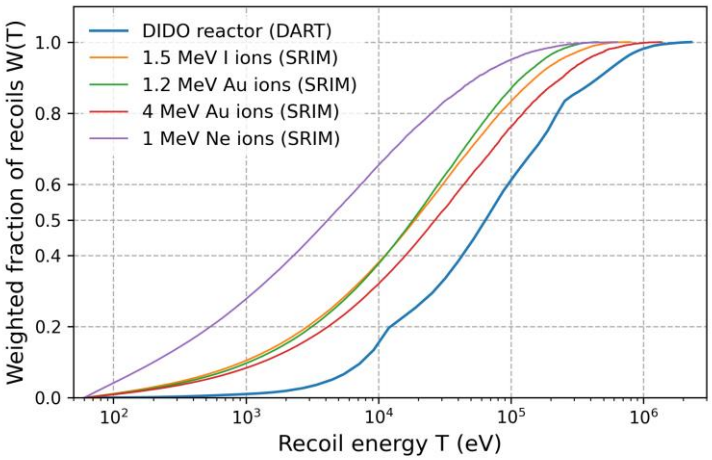

Figure 5: Weighted average recoil spectra corresponding to the neutron spectrum of the DIDO reactor and to 4 MeV Au^{2+}, 1.5 MeV I^+, 1.2 MeV Au^+ and 1 MeV Ne^+ ions; target is MgO.

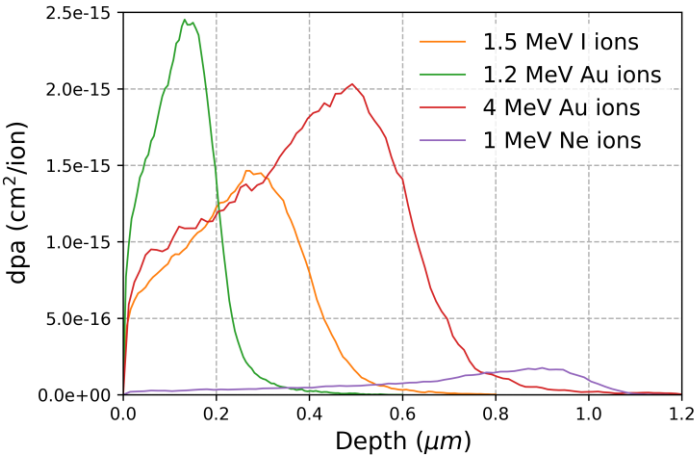

Figure 6: Dpa depth distributions corresponding to the three conditions implemented for the irradiation of the MgO single crystals, plus the profile corresponding to [55] (i.e. 1 MeV Ne). Calculations were performed with SRIM [36] using the FD mode.

Figure 7(a) shows XRD curves of MgO crystals irradiated with 4 MeV Au^{2+} ions (i.e. with the hardest WARS). Here, contrary to Ni, we do measure an elastic strain, as indicated by the appearance of a diffraction signal on the low-angle side of the XRD curves [16,37,45]. This strain is tensile, in agreement with the lattice expansion observed after irradiation in the DIDO reactor [46]. The strain magnitude as a function of dpa is plotted in Fig.8. Note that the strain was determined using the position of the interference fringe (i.e. the shoulder-like feature) on the low-angle side of the XRD patterns, as explained in [15]. Except at very low dpa (up to ~0.05), there is no match between the strain kinetics of neutron and 4 MeV Au irradiations. The lattice expansion is clearly more important in the case of the ion irradiation. Similarly, the strain build-up determined for 1.5 MeV I^{+} irradiations (see Fig. 7(b) for the XRD data) appears to be almost the same as that obtained for 4 MeV Au irradiations. As the corresponding WARS are very close, it is somehow not surprising to observe this similarity (despite the difference in the damage thickness). The strain kinetics derived from 1.2 MeV Au^{+} ion irradiations at 773 K (see [37] for XRD data) looks very different from the two previous mentioned ones, but extremely close to that obtained for neutron irradiation. Note that this particular temperature appears to be the most relevant one to get a close match, as clearly shown in Appendix C where strain build-ups for different temperatures are presented. A noticeable similarity of the strain kinetics of 1.2 MeV Au^{+} ions at 773 K with the one derived from the neutron irradiation is the limited strain level, even at the highest dpa. This finding cannot be explained by an annealing effect due to the electronic energy deposition, as this component is very close for all (Au and I) irradiations, i.e., in the range of 2 to 4 keV/nm (so relatively low [56]). Furthermore, the nuclear energy-loss component also lies in this range for the three cases, and, for ionizing events to affect the defect formation in MgO, the ratio of electronic to nuclear stopping power must be significantly larger than 1 [56]. In contrast, it has

been shown that temperature favors defect recombination in MgO [37,57], so the 773 K temperature can explain the limited lattice parameter change for the 1.2 MeV Au^+ irradiations. The fact that the corresponding strain build-up matches that of the neutron irradiations performed at 300 K strongly points to a dose rate effect. Indeed, as mentioned in section III, it is known that the difference in dpa rate between neutron and ion irradiation experiments can be accounted for by an increase in temperature during ion irradiation, so that the net defect fluxes during neutron irradiation are better reproduced. In the present case, it appears that a dynamic annealing must take place during neutron irradiation (because of the very low dpa rate), and the efficiency of this annealing process is achieved by significantly increasing the temperature (by ~473 K) during ion irradiation. A temperature shift of 3.5 times has been reported to account for a large difference in damage rates - on the order of 10^{12} - between experiments and molecular dynamics calculations in irradiated pyrochlores [58]. Here, the difference in dose rate between neutron and Au irradiations is on the order of 10^5, so a temperature shift of ~2.5 times for a material of the same class (ceramic oxide) appears plausible.

The lattice strain build-up obtained in [55] for 1 MeV Ne^+ irradiations appears to be very similar to those determined for 1.2 MeV Au at 773 K and neutron irradiations. An ionizing effect cannot be invoked to explain this resemblance, as the electronic energy loss for Ne experiments was less than 1 keV/nm. A likely explanation is rather related to the very soft WARS ($T_{1/2}$ is 4 keV as compared to 18.5 keV for 1.5 MeV I^+ ions and 26.8 keV for 4 MeV Au^{2+} ions). Indeed, it has been shown, by molecular dynamics simulations in a comparable ceramic oxide (namely UO_2), that the number of surviving Frenkel pairs is ~30, 120 and 180 for PKA energies of 4, 18 and 27 keV, respectively [28]. These values suggest (considering that the ion fluence ranges are similar) that the residual defect concentration is decreased by a factor 4 from iodine to neon irradiations, while it decreases only by 30 % from 4 MeV Au to iodine irradiations. Therefore, the strain level, which in this regime should be proportional to the defect density [37], is expected to not vary significantly between I and Au irradiations (as we do observe), whereas a substantial decrease is expected between I and Ne, as shown in Fig.8. Ergo, the agreement between the strain kinetics of 1 MeV Ne^+ irradiations and neutron irradiations also suggests that, in addition to the effective defect creation rate (that can be controlled by the dpa rate or the temperature), the PKA median energy should also be considered as a relevant parameter in defining the ion irradiation condition. This conclusion should hold for other materials as long as no microstructural change leading to strain relaxation (e.g. formation of dislocation lines, amorphization) takes place.

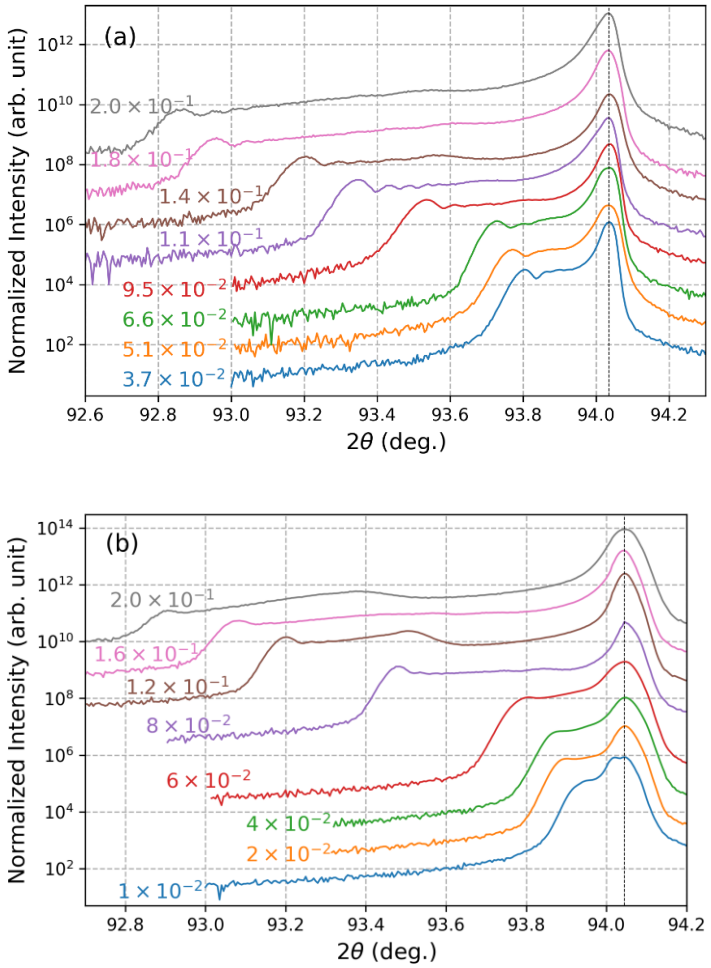

Figure 7: XRD curves of MgO single crystals irradiated with 1.5 MeV I^{+} ions (a) and with 4 MeV Au^{2+} ions (b) at the indicated dpa. The vertical dotted line indicates the position of the Bragg peak for the pristine crystal. Curves are stacked for visualization purposes.

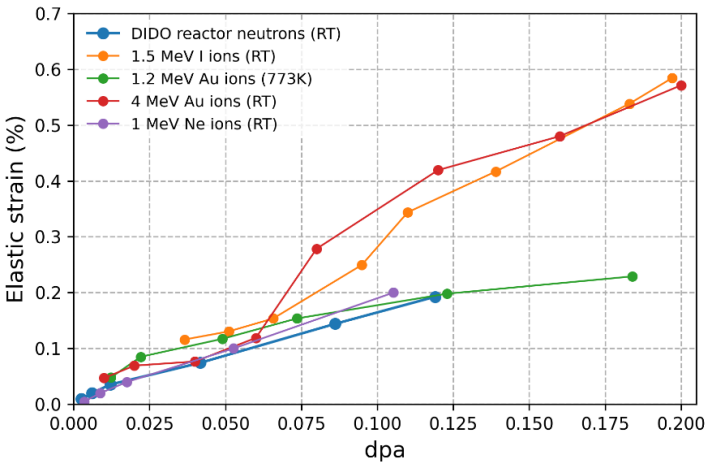

Figure 8: Elastic strain determined in irradiated MgO single crystals under the conditions indicated in the legend as a function of the dpa level determined with SRIM [36] using the FD mode.

Summary and conclusion

In this work, we performed ion irradiation experiments specifically designed to tentatively mimic selected neutron irradiations. We studied two materials, namely Ni and MgO (single crystals), for which there exists, in the literature, data of lattice parameter change (elastic strain) after irradiation in a nuclear reactor. The choice of the ion nature and energy was essentially dictated by the aim of having similar weighted average recoil spectra for ion and neutron irradiation experiments. We then performed HR-XRD measurements to monitor the strain build-up. We found that for Ni (and presumably any other pure metal), ion irradiation cannot allow, at least not with the adopted methodology, reproducing experimental results like the elastic strain developing upon neutron irradiation. The main reason for this failure lies in the defect spectrum produced upon ion irradiation that does not lead to a measurable strain. On the contrary, for MgO, ion irradiation can lead to similar results as those found after irradiation in a reactor, providing that the (ion) irradiation temperature is significantly increased in order to account for the large discrepancy in the damage creation rates. Therefore, choosing an *ad hoc* WARS is not sufficient to ensure perfectly mimicking neutrons with ions. Beside, we also show that, on the contrary, softening the WARS can have a similar effect as an increase in the temperature.

As a final remark, we would like to state that, as such a 'simple' comparison of the lattice parameter change between ion and neutron irradiation is not straightforward, perhaps ion irradiation should be considered as a mean to understand the basics of irradiation effects in materials rather than a proxy for neutron irradiation. Yet, if one wants to use ions to reproduce neutron effects, considering the corresponding WARS could be a way to improve the agreement between the two experiments.

Acknowledgments

XJ and AD would like to thank Laurence Luneville and David Simeone, CEA Paris-Saclay, for fruitful scientific discussions about the comparison between SRIM and DART codes. They also would like to express their gratitude to Viacheslav Chernov at the Bochvar Research Institute of Inorganic Materials (Moscow, Russia) for providing the neutron spectrum of the IVV-2M reactor. Part of this work has been funded by the NEEDS program of the CNRS (project MeSINII).

References

[1] G. Was, J. Mater. Research 30 (2015) 1158.

[2] S. J. Zinkle, L. L. Snead, Scripta Mater. 143 (2018) 154.

[3] M. Roldán, P. Galán, F. J. Sánchez, I. García-Cortés, D. Jiménez-Rey, Pilar Fernández, IntechOpen, Online First (2019), DOI: 10.5772/intechopen.87054.

[4] L. K. Mansur, J. Nucl. Mater. 206 (1993) 306.

[5] C. Abromeit, J. Nucl. Mater. 216 (1994) 78.

[6] O. V. Ogorodnikova, V. Gann, J. Nucl. Mater. 460 (2015) 60.

[7] N. Galy, N. Toulhoat, N. Moncoffre, Y. Pipon, N. Bérerd, M. R. Ammar, P.Simon, D. Deldicque, P. Sainsot, J. Nucl. Mater. 502 (2018) 20.

[8] R. W. Harrison, Vacuum 160 (2019) 355.

[9] L. L. Snead, Y. Katoh, T. Koyanagi, K. T. Eliot, D. Specht, J. Nucl. Mater. 471 (2016) 92.

[10] S. Jublot-Leclerc, X. Li, L. Legras, M.-L. Lescoat, F. Fortuna, A. Gentils, J. Nucl. Mater. 480 (2016) 436.

[11] Z. Jiao, J. Michalicka, G. S. Was, J. Nucl. Mater. 501 (2018) 312.

[12] M. Hernández Mayorala, F. Bergner, C. Heintze, V. Kuksenko, C. Pareige, Ph. Pareige, L. Malerba, NEA-NSC-WPFD-DOC--2015-9 (RN:46040920).

[13] Ce Zheng, M. A. Auger, M. P. Moody, D. Kaoumi, J. Nucl. Mater. 491 (2017) 162.

[14] A. Debelle, J. Channagiri, L. Thomé, B. Décamps, A. Boulle, S. Moll, F. Garrido, M. Behar, J. Jagielski, J. Appl. Phys 115 (2014) 183504.

[15] A. Debelle, A. Declémy, Nucl. Instr. and Methods B 268, (2010) 1460.

[16] A. Boulle, V. Mergnac, J. Appl. Crystal. 53 (2020) 587.

[17] J.C. Haley, S. de Moraes Shubeita, P. Wady, A.J. London, G.R. Odette, S. Lozano-Perez, S.G. Roberts, J. Nucl. Mater. 533 (2020) 152130.

[18] E.H. Megchiche, S. Pérusin, J-C Barthelat, C. Mijoule, Phys. Rev. B 74 (2006) 064111.

[19] B. P. Uberuaga, R. Smith, A. R. Cleave, G. Henkelman, R. W. Grimes, A. F. Voter, K. E. Sickafus, Phys. Rev. B 71 (2005) 104102.

[20] F.A. Garner, J. Nucl. Mater. 117 (1983) 177.

[21] O. Tissot, C. Pareige, E. Meslin, B. Décamps, J. Henry, Mater. Res. Letters 5 (2017) 117.

[22] P.J. Burnett, T.F. Page, Radiat. Eff. 97 (1986) 283.

[23] D. Misra, S. K Yadav, arXiv preprint arXiv:1901.05607.

[24] B. Canut, J.P. Dupin, L. Gea, S.M.M. Ramos, P.Thevenard, NIM B 59-60 (1991) 1211.

[25] A. V. Fedorov, M.A. Huis, A Van Veen, H. Schut, NIM B 166-167 (2000) 215.

[26] T. Aruga, Y. Katano, T. Ohmichi, S. Okayasu, Y. Kazumata, S Jitsukawa, NIM B 197 (2002) 94.

[27] R. S. Averback, R. Benedek, K. L. Merkle, Phys. Rev. B 18 (1978) 4156.

[28] J-P Crocombette, L. Van Brutzel, D. Simeone, L. Luneville, J. Nucl. Mater. 474 (2016) 134.

[29] C. J. Ortiz, Comp. Mater. Science 154 (2018) 325.

[30] K. Nordlund, A. E. Sand, F. Granberg, S. J. Zinkle, R. Stoller, R. S. Averback, T. Suzudo, L. Malerba, F. Banhart, W. J. Weber, F. Willaime, S. Dudarev, D. Simeone, J. Nucl. Mater. 512 (2018) 450.

[31] R. S. Averback, J. Nucl. Mater. 216, 49 (1994).

[32] L. Lunéville, D. Simeone, C. Jouanne, J. Nucl. Mater. 353 (2006) 89.

[33] M. T. Robinson, Rad. Effects and Defect in Solids Null (1994) 3.

[34] W. Eckstein, The Binary Collision Model in "Computer Simulation of Ion-Solid Interactions", p.4, Springer, Berlin, Heidelberg, 1991.

[35] G. S. Was, Fundamentals of Radiation Materials Science: Metals and Alloys (Berlin: Springer) 2007.

[36] J. F. Ziegler, J. P. Biersack, U. Littmark, The Stopping and Range of Ions in Solids, Pergamon, New York, 1985. SRIM program can be downloaded at: www.srim.org.

[37] D. Bachiller-Perea, A. Debelle, L. Thomé, J.-P. Crocombette, J. Mater. Sci. 51 (2016) 1456.

[38] K. Nordlund, S. J. Zinkle, A. E. Sand, F. Granberg, R. S. Averback, R. Stoller, T. Suzudo, L. Malerba, F. Banhart, W. J. Weber, F. Willaime, S. L. Dudarev, D. Simeone, Nature Comm. 9 (2018) 1084.

[39] L. Luneville, D. Simeone, D. Gosset, Nucl. Instr. and Methods B 250 (2006) 71.

[40] J. Lindhard, Phys. Rev. B 14 (1961) 1.

[41] R. E. Stoller, M. Toloczko, G. S. Was, Nucl. Instr. and Methods B 310 (2013) 75.

[42] J-P Crocombette, C. Van Wambeke, EPJ Nuclear Sci. Technol. 5 (2019) 7.

[43] W. J. Weber, Y. Zhang, Current Opinion Solid State and Materials Science 23 (2019) 100757.

[44] S. I. Rao, C. R. Houska, J. Mater. Sci. 25 (1990) 2822.

[45] A. Debelle, A. Boulle, F. Rakotovao, J. Moeyaert, C. Bachelet, F. Garrido, L. Thomé, J. Phys. D: Appl. Phys. 46, (2013) 045309.

[46] V. I. Voronin, I. F. Berger, N. V. Proskurnina, B. N. Goschitskii, The Physics of Metals and Metallography 117 (2016) 348.

[47] O Bender, P Ehrhart, J. Phys. F: Met. Phys. 13 (1983) 911.

[48] R. J. Olsen, Ke Jin, C. Lu, L. K. Beland, L. Wang, H. Bei, E. D. Specht, B. C. Larson, J. Nucl. Mater. 459 (2016) 153.

[49] N. Sellami, A. Debelle, M. W. Ullah, H. M. Christen, J. K. Keum, H. Bei, H. Xue, W. J. Weber, Y. Zhang, Current Opinion in Solid State and Materials Science 23 (2019) 107.

[50] B. C. Larson, J. Appl. Phys. 45 (1974) 514.

[51] V. Speriosu, B. M. Paine, M-A. Nicolet, H. L. Glass, Applied Physics Letters 40 (1982) 604.

[52] A. Debelle, J.-P. Crocombette, A. Boulle, A. Chartier, Th. Jourdan, S. Pellegrino, D. Bachiller-Perea, D. Carpentier, J. Channagiri, T.-H. Nguyen, F. Garrido, L. Thomé, Phys. Rev. Mater. 2 (2018) 013604.

[53] B. Henderson, D. H. Bowens, J. Phys. C: Solid St. Phys. 4 (1971) 1487.

[54] S.J. Zinkle, C. Kinoshita, J. Nucl. Mater. 251 (1997) 200.

[55] A. I. Van Sambeek, R. S. Averback, Mat. Res. Soc. Symp. Proc. Vol. 396 (1996) 137.

[56] S. J. Zinkle, NIM B 91 (1994) 234.

[57] A. Debelle, J.-P. Crocombette, A. Boulle, E. Martinez, B. P. Uberuaga, D. Bachiller-Perea, Y. Haddad, F. Garrido, L. Thomé, M. Béhar, Phys. Rev. Mater. 2 (2018) 083605.

[58] J-P Crocombette, A. Chartier, W. J. Weber, Appl. Phys. Lett. 88 (2006) 051912.

Table I: Detailed characteristics of neutron and ion irradiations – case of Ni crystals

IVV-2M neutron reactor		**300 keV Bi^{2+} ions**		**600 keV Ni^{+} ions**	
fluence (cm^{-2})	dpa	fluence (cm^{-2})	dpa	fluence (cm^{-2})	dpa
$1.0x10^{18}$	$4.3x10^{-4}$	$3.6x10^{10}$	$5x10^{-4}$	$2.15x10^{11}$	$8.7x10^{-4}$
$1.0x10^{19}$	$4.3x10^{-3}$	$3.6x10^{11}$	$5x10^{-3}$	$2.15x10^{12}$	$8.7x10^{-3}$
$5.0x10^{19}$	$2.15x10^{-2}$	$1.8x10^{12}$	$2.5x10^{-4}$	$1.1x10^{13}$	$4.3x10^{-2}$
$1.0x10^{20}$	$4.3x10^{-2}$	$3.6x10^{12}$	$5x10^{-2}$	$2.15x10^{13}$	$8.7x10^{-2}$

Table II: Detailed characteristics of neutron and ion irradiations – case of MgO crystals

DIDO neutron reactor		**1.5 MeV I^{+} ions**		**1.2 MeV Au^{+} ions**		**4 MeV Au^{2+} ions**	
fluence (cm^{-2})	dpa	fluence (cm^{-2})	dpa	fluence (cm^{-2})	dpa	fluence (cm^{-2})	dpa
$1.7x10^{18}$	$2.5x10^{-3}$	$2.5x10^{13}$	$3.65x10^{-2}$	$5.0x10^{12}$	$1.25x10^{-2}$	$4.9x10^{12}$	$1.0x10^{-2}$
$4.1x10^{18}$	$6.1x10^{-3}$	$3.5x10^{13}$	$5.1x10^{-2}$	$9.0x10^{12}$	$2.2x10^{-2}$	$9.9x10^{12}$	$2.0x10^{-2}$
$8.1x10^{18}$	$1.2x10^{-2}$	$4.5x10^{13}$	$6.6x10^{-2}$	$2.0x10^{13}$	$4.9x10^{-2}$	$2.0x10^{13}$	$4.0x10^{-2}$
$2.8x10^{19}$	$4.15x10^{-2}$	$6.5x10^{13}$	$9.5x10^{-2}$	$3.0x10^{13}$	$7.35x10^{-2}$	$3.0x10^{13}$	$6.0x10^{-2}$
$5.8x10^{19}$	$8.6x10^{-2}$	$7.5x10^{13}$	$1.1x10^{-1}$	$5.0x10^{13}$	$1.25x10^{-1}$	$3.9x10^{13}$	$8.0x10^{-2}$
$8.0x10^{19}$	$1.2x10^{-1}$	$9.5x10^{13}$	1.410^{-1}	$7.5x10^{13}$	$1.85x10^{-1}$	$5.9x10^{13}$	$1.2x10^{-1}$
		$1.25x10^{14}$	$1.8x10^{-1}$			$7.9x10^{13}$	$1.6x10^{-1}$
		$1.35x10^{14}$	$1.95x10^{-1}$			$9.9x10^{13}$	$2.0x10^{-1}$

Appendix A: Neutron spectra in the IVV-2M and DIDO nuclear reactors

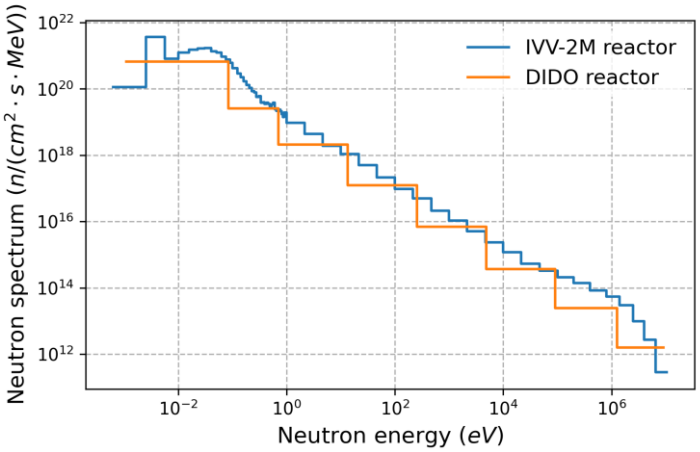

Appendix B: Lattice parameter change (elastic strain) in Ni single-crystals irradiated in the IVV-2M nuclear reactor

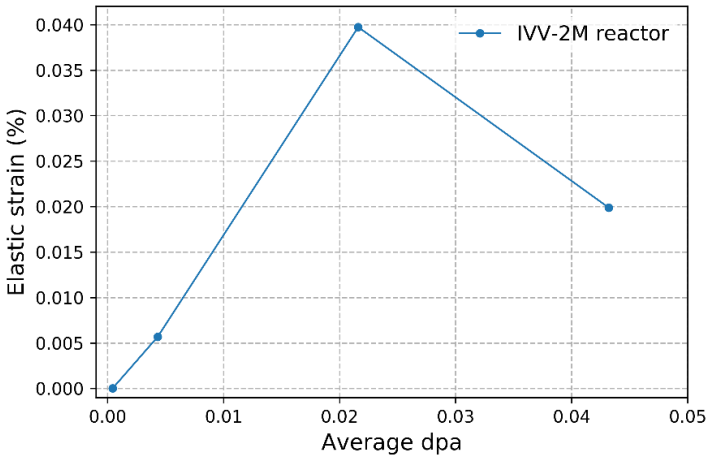

Appendix C: Lattice parameter change (elastic strain) in MgO single-crystals irradiated with 1.2 MeV Au^+ ions at different temperatures